ISBN: 978-3-95450-227-1 ISSN: 2673-5490 doi:10.18429/JACoW-IPAC2022-WEPOMS057

SIMULATION STUDIES AND MACHINE LEARNING APPLICATIONS AT THE COHERENT ELECTRON COOLING EXPERIMENT AT RHIC*

W. Lin[1,†], M. A. Sampson[1], Y.C. Jing[2], K. Shih[3], G. H. Hoffstaetter[1,2], J. A. Crittenden[1]
[1]CLASSE, Cornell University, Ithaca, New York, USA
[2]Collider-Accelerator Department, Brookhaven National Laboratory, Upton, New York, USA
[3]Physics Department, Stony Brook University, New York, USA

Abstract

Coherent electron cooling is a novel cooling technique which cools high-energy hadron beams rapidly by amplifying the modulation induced by hadrons in electron bunches. The Coherent electron cooling (CeC) experiment at Brookhaven National Laboratory (BNL) is a proof-of-principle test facility to demonstrate this technique. To achieve efficient cooling performance, electron beams generated in the CeC need to meet strict quality standards. In this work, we first present sensitivity studies of the low energy beam transport (LEBT) section, in preparation for building a surrogate model of the LEBT line in the future. We also present preliminary test results of a machine learning (ML) algorithm developed to improve the efficiency of slice-emittance measurements in the CeC diagnostic line.

INTRODUCTION

The layout of the current CeC system is shown in Fig. 1. The electrons are generated from the superconducting radio frequency (SRF) gun with 1.5 nC of charge per bunch, and then bunched with a normal conducting RF cavity. The electron bunches are compressed ballistically in a long drift and accelerated to 14.5 MeV at the end of the low energy beam transport (LEBT) section [1]. To perform cooling, the accelerated electron beam travels through the dog-leg to interact with ions in the common section with RHIC. To evaluate electron beam quality, the transverse deflecting cavity (TDC) in the diagnostic line converts the electron beam's longitudinal distribution into a transverse distribution, which is measurable via YAG screens.

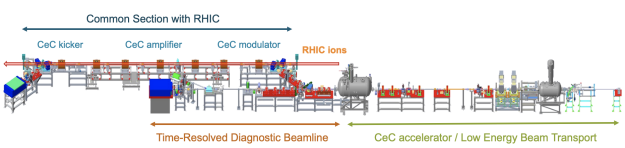

Figure 1: Current CeC system layout at BNL. Electron beams travel from right to left.

Electron beams need to meet strict requirements in the CeC accelerator and in the LEBT section to achieve efficient cooling performance in the common section with RHIC. Therefore, understanding how electron beam profiles are controlled and measured in the CeC system is crucial.

* Work supported by the U.S. National Science Foundation under Award PHY-1549132, and by Brookhaven Science Associates, LLC under Contract No. DEAC0298-CH10886 with the U.S. Department of Energy.
† wl674@cornell.edu

SENSITIVITY STUDIES OF LOW ENERGY BEAM TRANSPORT

A start to end (S2E) simulation of the low energy beam transport (LEBT) section was established using the beam dynamics code IMPACT-T [2]. There are three RF cavity systems (112 MHz SRF gun, 500 MHz buncher, and 704 MHz 5-cell SRF linac) and 6 solenoids (1 gun solenoid, 5 LEBT solenoids) in the LEBT beam line. The IMPACT-T simulation uses all components to optimize the electron beam profile at the end of the LEBT section, aiming for high peak current and low slice emittance for the core of the beam. The optimization results are summarized in [3].

To obtain core emittance measurements, the final electron beam from the IMPACT-T simulation is sliced longitudinally from the center by a Python script, and grouped into 20%, 50%, 80%, and 100% of the total particles. The script then calculates the normalized emittance for each group, and the emittance and current for each longitudinal slice, and plots all the results in an image. One sample image from the Python script is presented in Fig. 2.

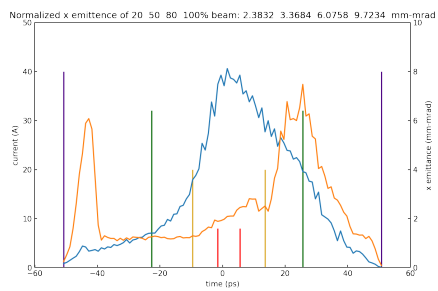

Figure 2: Slice current (blue) and slice emittance (orange) results for the electron beam at the end of the LEBT section. The emittances for the central 20% (red), 50% (yellow), 80% (green), and 100% (purple).

The end goal of the studies was to identify which control parameters are important to the beam behavior, so that they can be included in a neural network surrogate model for the LEBT section.

Table 1 lists the parameters considered in this project, and the value ranges within which they were changed. The SRF gun, gun solenoid, and the buncher are not included because the initial beam distribution used to run the studies in IMPACT-T already included effects from known displacement errors from the gun to the buncher.

In this work, sensitivity is defined as the effect a control parameter has on the core emittance of the electron beam,

ISBN: 978-3-95450-227-1 ISSN: 2673-5490 doi:10.18429/JACoW-IPAC2022-WEPOMS057

Table 1: LEBT Control Parameters Scan Range

Name	Unit	Range
SRF Linac voltage	V	$2.398 \times 10^7 \pm 5\%$
SRF Linac phase	deg	$239.1 \pm 1.5°$
LEBT Solenoid 1 strength	T	$0.033 \pm 1\%$
LEBT Solenoid 2 strength	T	$-0.036 \pm 1\%$
LEBT Solenoid 3 strength	T	$0.035 \pm 1\%$
LEBT Solenoid 4 strength	T	$-0.038 \pm 1\%$
LEBT Solenoid 5 strength	T	$0.047 \pm 1\%$
SRF Linac x displacement	mm	[-5,5]
SRF Linac y displacement	mm	[-5,5]

calculated using Eq. (1). The 50% emittance is used as core emittance. We ran the LEBT IMPACT-T simulation multiple times, each time with only one control parameter set at a different value within its designated range. The final electron beam distribution is extracted from the simulation and analyzed by the Python script to obtain its slice emittance.

$$\text{sensitivity} = \frac{d(50\%\ \text{emittance})}{d(\text{parameter})} \tag{1}$$

Table 2 shows the calculated results for all control parameters using Eq. (1). We see that solenoids have the biggest impacts on the emittance profile, which is expected since they are the major components used to adjust the phase space beam distribution, so that all longitudinal beam slices are well aligned to give minimum projected emittance at the end of the LEBT section, as described in [3].

Table 2: Sensitivity of LEBT Control Parameters

Name	Slope
SRF Linac voltage	-2.34×10^{-8} mm-mrad/V
SRF Linac phase	-0.031 mm-mrad/deg
LEBT Solenoid 1 strength	559 mm-mrad/T
LEBT Solenoid 2 strength	-304 mm-mrad/T
LEBT Solenoid 3 strength	-444 mm-mrad/T
LEBT Solenoid 4 strength	-314 mm-mrad/T
LEBT Solenoid 5 strength	499 mm-mrad/T
SRF Linac x displacement	-0.023 mm-mrad/mm
SRF Linac y displacement	0.028 mm-mrad/mm

EMITTANCE MEASUREMENT IN THE DIAGNOSTIC BEAM LINE

In the actual CeC system, the horizontal slice emittances of the electron beam are measured in the time-resolved diagnostic beam line with the quadrupole scan method [4]. In the CeC diagnostic line, the transverse deflecting cavity tilts the beam upward so that the longitudinal coordinate is depicted vertically on the screen, provided the vertical beam size is narrowly focused. Figure 3 illustrates the setup for this method.

The traditional quadrupole scan method uses only one quadrupole, which would bring the vertical beam size out of focus on the screen. To ensure vertical beam focusing is maintained during the scan, two quadrupoles, Q3 and Q4, are used with opposite polarity.

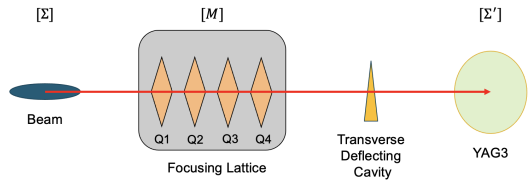

Figure 3: Beam line setup to measure horizontal slice emittances with the quadrupole scan method.

In Fig. 3, Σ and Σ' are the 2nd order beam-moment matrices for the electron beam at the beginning of the diagnostic line and at the YAG screen, and M is the transfer matrix for that section. The beam matrix at the screen can be calculated as $\Sigma' = M\Sigma M^T$. The CeC diagnostic line focuses on measuring the horizontal emittance, so all matrices are in two dimensional transverse phase space. Focusing on the (1, 1) element of Σ', we have:

$$\sigma'_{11} = m_{11}^2\sigma_{11} + m_{11}m_{12}2\sigma_{12} + m_{12}^2\sigma_{22} \tag{2}$$

$$\frac{\sigma'_{11}}{m_{12}^2} = \sigma_{11}\left(\frac{m_{11}}{m_{12}}\right)^2 + 2\sigma_{12}\left(\frac{m_{11}}{m_{12}}\right) + \sigma_{22} \tag{3}$$

Using Eq. (3), we measure a series of beam sizes σ'_{11} for different values of $1/m_{12}^2$ and of m_{11}/m_{12} during the quadrupole scan and fit a parabola to the data to obtain σ_{11}, σ_{12}, and σ_{22}. The RMS emittance of the electron beam at the beginning of the diagnostic line is then $\varepsilon = \sqrt{\sigma_{11}\sigma_{22} - \sigma_{12}^2}$.

The current emittance measurement routine finds best focusing Q3 – Q4 combinations by sequential scans. While a vertically focusing quadrupole combination can easily be found for linear optics, it can't easily be predicted when space-charge forces are involved. Thirteen Q3 settings within a preset range are scanned. For each Q3 setting, nine Q4 setting are scanned, and the Q3 – Q4 combination that gives the best vertical focusing (smallest vertical RMS beam size) is saved for emittance calculation. One sample plot saved from a quadrupole scan performed on March 25 is shown in Fig. 4. Due to the large number (> 100) of measurements needed for one complete scan, this routine takes more than 1 hour to complete. We set out to use machine learning to implement a faster alternative.

To speed up the quadrupole scan routine, we proposed a new routine that incorporates a machine learning technique. Neural networks (NNs) are computing systems capable of recognizing underlying relationships between data sets and make fast and accurate models [5]. We train a NN with CeC diagnostic line data, so it can establish a mapping between quadrupole settings and beam size. With sufficient training, the NN model can predict electron beam behavior accurately with any given quadrupole settings, and we can use it to find

ISBN: 978-3-95450-227-1 ISSN: 2673-5490 doi:10.18429/JACoW-IPAC2022-WEPOMS057

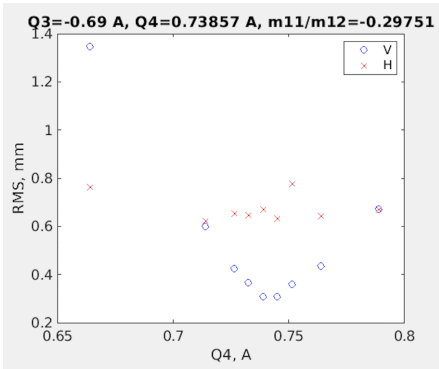

Figure 4: Sample historical results from a quadrupole scan.

the best Q3 – Q4 combinations much faster than the current scan method.

The new quadrupole scan routine is outlined as the following:

1. Use the old quadrupole scan routine to scan 6 Q3 settings. With 9 Q4 scans for each Q3 scan, we obtain 54 data points from the real CeC diagnostic line system.

2. We use the saved 54 data points to train a neural network (NN) model, with Q3 and Q4 settings as inputs and vertical RMS beam sizes as outputs.

3. After training, we give the NN model the remaining 7 Q3 settings that need to be scanned.

4. The NN model predicts corresponding Q4 settings that would give the smallest vertical RMS beam sizes.

5. We save the predicted Q3 – Q4 combination and load them one by one to the real beam line, and record the actual beam sizes.

We tested the new quadrupole scan routine on the CeC diagnostic line, and the results are shown in Fig. 5 and Fig. 6. The actual beam sizes are in blue and the NN predicted beam sizes are in orange.

Figure 5 shows the training results of the NN model from the first 54 data points. The NN model was able to recognize the general parabolic pattern of the beam size behavior, however, it has some difficulties getting accurate predictions for the smaller beam sizes. This inaccuracy can be caused by various reasons, which requires further investigations and adjustments. One possible reason is that the algorithm focuses too much on getting the maxima right, while we care more about the minima. This can be fixed by either using only smaller values to train, or implementing a weighted loss function [6] during training so the model puts more emphasis on accuracy for small values. Another possible solution is to simply reverse the signs of the data, which can test whether NN model performs better when most data is centered around the maxima rather than the minima.

Despite the fact that the NN model was not perfectly trained to capture the real diagnostic line behavior, we still

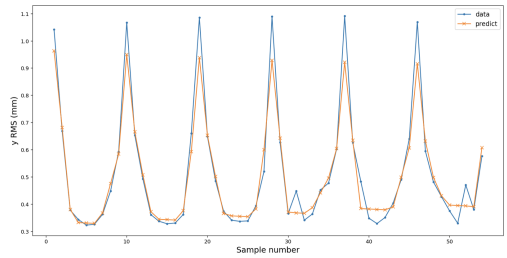

Figure 5: Neural network (NN) model training results using 54 training data points.

obtained satisfactory results for the 7 prediction rounds, as shown in Fig. 6. Using the predicted Q3 – Q4 settings, the actual RMS beam sizes measured in the real system are all within the 0.3 – 0.45 mm range, which agrees with the optimal vertical RMS beam sizes recorded from previous quadrupole scans using the old routine. The NN predicted beam sizes are also all within 13% error from the real beam sizes, which is decent considering the trouble we encountered during training. With this new routine, the emittance measurement time is decreased by at least 50%.

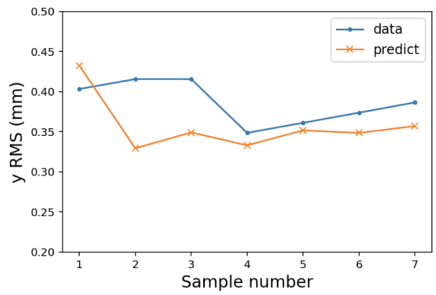

Figure 6: Vertical beam sizes from 7 quadrupole settings generated by the NN model.

For future work, we aim to include more input parameters (e.g., trim magnet settings) into the NN model, to better capture the complex nature of the CeC beam line. This should help with improving the accuracy of the NN model. We will also work on better incorporating the new routine into the CeC control system, as the current method requires a cumbersome switch between two different scripts.

CONCLUSION

We conducted sensitivity studies in the CeC low energy beam transport section and also tested using neural networks to speed up the slice emittance quadrupole scan in the diagnostic beam line. The sensitivity studies agree with the previous simulation studies and lay a foundation for building future surrogate model for the LEBT section. The new quadrupole scan routine with NN model is proven experimentally to be efficient in cutting the scan time by 50% or more. This work demonstrate that it can have significant benefits to incorporate machine learning algorithms into an accelerator control system.

ISBN: 978-3-95450-227-1 ISSN: 2673-5490 doi:10.18429/JACoW-IPAC2022-WEPOMS057

REFERENCES

[1] V. Litvinenko *et al.*, "Coherent Electron Cooling (CeC) Experiment at RHIC: Status and Plans," in *Proc. IPAC'19*, Melbourne, Australia, May 2019, pp. 2101–2104, doi:10.18429/JACoW-IPAC2019-TUPTS078

[2] J. Qiang, "IMPACT-T: A 3D Parallel Particle Tracking Code in Time Domain," https://amac.lbl.gov/~jiqiang/IMPACT-T/index.html

[3] Y. C. Jing, V. Litvinenko, I. Petrushina, I. Pinayev, K. Shih, and Y. H. Wu, "Beam Dynamics in Coherent Electron Cooling Accelerator," in *Proc. IPAC'21*, Campinas, Brazil, May 2021, pp. 4216–4218, doi:10.18429/JACoW-IPAC2021-THPAB219

[4] M. G. Minty and F. Zimmermann, "Measurement and control of charged particle beams," in 2003, ch. 4.1, pp. 99–116, ISBN: 9783540441878.

[5] O. I. Abiodun, A. Jantan, A. E. Omolara, K. V. Dada, N. A. Mohamed, and H. Arshad, "State-of-the-art in artificial neural network applications: A survey," *Heliyon*, vol. 4, no. 11, e00938, 2018, doi:10.1016/j.heliyon.2018.e00938

[6] K. R. M. Fernando and C. P. Tsokos, "Dynamically weighted balanced loss: Class imbalanced learning and confidence calibration of deep neural networks," *IEEE Transactions on Neural Networks and Learning Systems*, pp. 1–12, 2021, doi:10.1109/TNNLS.2020.3047335